

THE LOCAL TIME DEPENDENCE OF THE NON-STÖRMER CUT-OFF
FOR 1.5 MeV PROTONS IN THE QUIET GEOMAGNETIC FIELD*†

Edward C. Stone (*Ph.D. Thesis*) Feb. 1964 498
 ② Enrico Fermi Institute for Nuclear Studies and
 Department of Physics
 ① University of Chicago U. S. A.
 Chicago 37, Illinois
refer
Submitted
for
Publication

0591032

Submitted to
 Journal of Geophysical Research
 February 1964

NASA Grant NSG-179-61; Contract

* This research was supported in part by the Air Force Office of Scientific Research under contract AF 49 (638)-1008 and grant AF-AFOSR-62-23) and by the National Aeronautics and Space Administration under grant NASA-NsG-179-61.

† A thesis submitted to the Department of Physics, the University of Chicago, Chicago, Illinois, in partial fulfillment of the requirements for the Ph.D. degree.

+ NASA Fellow.

Present address: California Institute of Technology, Pasadena, California

THE LOCAL TIME DEPENDENCE OF THE NON-STÖRMER CUT-OFF¹
FOR 1.5 MeV PROTONS IN THE QUIET GEOMAGNETIC FIELD*[‡]

Edward C. Stone⁺
Enrico Fermi Institute for Nuclear Studies
and Department of Physics
University of Chicago
Chicago 37, Illinois

184 37 ABSTRACT A

Two solid state detector telescopes, vertically and horizontally oriented, were launched into a polar orbit during a time of low geomagnetic activity. A small flux of 1.5 MeV protons, interacting with the geomagnetic field as individual particles, was observed at all latitudes above a characteristic cut-off latitude. The observed vertical cut-off was 65° on the night side and 67° on the day side, as compared to a theoretical Störmer cut-off of 76° . The local time dependence was also apparent in the cut-off transition width characterized by the difference in the latitude at which the flux is first detectable and the latitude at which the maximum (plateau) flux is first observed. On the night side, the transition width was $\sim 1^{\circ}$, while on the day side the transition was $\sim 3^{\circ}$ and variable. The horizontal cut-off latitudes were similar. Essentially identical results were obtained over North and South Poles. These results not only provide a severe test for presently postulated cut-off theories, but they also suggest a re-examination of the proton flux spectra associated with polar cap blackout and polar cap absorption.

A UT 4 OR

* This research was supported in part by the Air Force Office of Scientific Research under contract AF 49 (638)-1008 and grant AF-AFOSR-62-23, and by the National Aeronautics and Space Administration under grant NASA-NsG-179-61.

[‡] A thesis submitted to the Department of Physics, the University of Chicago, Chicago, Illinois, in partial fulfillment of the requirements for the Ph.D. degree.

⁺ NASA Fellow

Present address: California Institute of Technology, Pasadena, California.

INTRODUCTION

An adequate understanding of ionospheric and cosmic ray phenomena in the polar regions is limited by a lack of information about the configuration of the geomagnetic field and its effect on these phenomena. The polar magnetic field can be studied by observing low energy, solar flare proton penetration through the magnetic field and into the ionosphere and upper atmosphere. Information about the effects of magnetic storms and the solar wind on the geomagnetic field can be obtained by comparing the observed penetration with that predicted by Störmer theory, which states that protons with a given energy (or rigidity) can reach the earth's atmosphere at all latitudes above a rigidity-dependent cut-off latitude.

The penetration of solar protons into the polar region has been studied in two periods: during magnetically quiet times just prior to the sudden commencement (called SC) of magnetic storm activity which often follows one to two days after particle-producing solar flares; and during the main phase of a geomagnetic storm, when the magnetic field disturbance severely alters the rigidity-dependent cut-off latitudes. The present observation occurred during a magnetically quiet period which was neither immediately preceded nor followed by magnetic storm activity.

For some time, the incidence of solar flare protons into the polar cap regions prior to SC has been inferred from increased absorption of radio frequency radiation (see Table I). Pre-SC radio absorption characteristically is observed only at geomagnetic latitudes greater than 65° (the polar cap region). However, radio absorption techniques have not defined the low latitude extent (or edge) of this region precisely. In addition, the energy and flux of protons producing the absorption are not measured directly but are derived theoretically, often assuming that the latitude of the edge is the cut-off latitude for 10 - 20 MeV protons.

Recent estimates indicate that proton fluxes $\geq 500 \text{ cm}^{-2} \text{ sec}^{-1} \text{ sr}^{-1}$ (Freier and Webber, 1963) are responsible for the observed absorption.

Direct observations from a satellite in the polar region prior to sudden commencement also indicate a cut-off latitude of $\sim 65^\circ$ for 1.5 - 15 MeV protons, as summarized in Table II. These July 1961 measurements showed a gradual increase in count rate between the threshold latitude of $\sim 65^\circ$ and the plateau latitude of $\sim 72^\circ$. The threshold latitude is the lowest latitude where they observed $> 10 \text{ protons/cm}^2 \text{ sec sr}$; the plateau latitude is the lowest latitude above which the flux is essentially constant. The wide energy interval (1.5 - 15 MeV) prevented any interpretation of the nature of this transition from threshold latitude to plateau latitude. The pre-SC count rate plateaus, corresponding to proton fluxes $\geq 300 \text{ cm}^{-2} \text{ sec}^{-1} \text{ sr}^{-1}$, extended at least to 78° , the maximum latitude attained by Injun I satellite. Although Injun I tumbled, preventing specific directional measurements, the flux was found isotropic over π steradians.

In the present experiment, these cut-off effects are investigated with two solid state detector telescopes which were vertically and horizontally oriented and provided specific directional and spectral information. The detectors were operated with a narrow energy window for protons and with virtually no electron sensitivity. The satellite tape recorder provided full coverage of data from both polar regions.

Three fortuitous circumstances add considerably to the importance of this measurement:

- 1) A 1.5 - 4.4 MeV proton flux of the order of $4 \text{ cm}^{-2} \text{ sec}^{-1}$ was present in the polar region in the first 8 orbits (through 0900 UT, 18 Sept. '61).

This is the first reported non-storm observation of a flux which is far below the critical flux level of $\sim 200 \text{ cm}^{-2} \text{ sec}^{-1}$ above which collective particle motion occurs in the geomagnetic field (Obayashi and Hakuru, 1961, after Ferraro, 1952).

2) The flux increased ten-fold after 0900 UT on September 18. The increased flux level was just large enough to be detected by Bryant, Cline, Desai and McDonald (1963) on Explorer XII satellite beyond $\sim 10 R_e$. Bryant, et. al. (1963) have pointed out similarities with other recurrent extraterrestrial proton events of solar origin.

3) The boundary of the geomagnetic field was observed at $> 13.5 R_e$ and at $12 R_e$ on 18 September 1961 and 19 September 1961, respectively, and the field inside was essentially regular (Cahill, private communication, 1963). Similarly, ground-based observations (Lincoln, 1962, a,b,c) show no magnetic storms and little magnetic activity.

All of the above circumstances made the following conclusions possible. During a magnetically quiet time, the entire North and South polar cap regions were accessible to 1.5 MeV protons. This region extended down to 65° geomagnetic latitude on the night side of the earth, with a transition width (the range in latitude in which the flux drops from maximum to the threshold of detection) of $\sim 1^\circ$ in latitude. However, on the day side this region extended down to 67° . The day side transition width was $\sim 3^\circ$ and variable. These results should be compared to the Störmer cut-off latitude of $\sim 76^\circ$ for 1.5 MeV protons, independent of local time. Since there was no unusual magnetic activity during the present observation, the large reduction in cut-off latitude is difficult to explain by any presently postulated cut-off theories. In addition, the very low cut-off latitude suggests the re-examination

of the proton fluxes responsible for pre-SC polar cap blackout and polar cap absorption.

Preliminary results have been reported elsewhere (Fan, Simpson, and Stone, 1964).

INSTRUMENTATION

The particle detectors were surface barrier solid state (AuSi) diodes prepared at the Laboratory for Applied Sciences of the University of Chicago. Typical characteristics are listed in Table III. Four detectors were used, two in each of the perpendicularly oriented telescopes. The configuration of detectors and aluminum collimator illustrated in Figure 1 was originally developed for the Ranger I and II spacecrafts (Takaki, Perkins, and Tuzzolino, 1961).

The orientation of the two telescopes (Figure 2) in the polar region was such that the vertical telescope detected only particles which would have been absorbed in the atmosphere, while the horizontal telescope responded mainly to particles which would have mirrored above the atmosphere (i.e., above ~ 100 km).

Figure 3 shows the calculated response of the detectors for perpendicularly incident protons and alphas. A 0.25 mil aluminized mylar light shield in front of the detectors reduced the response to protons with < 1 MeV. The electronic thresholds on the rate discriminators are shown in Figure 3. Two different discrimination levels were available on three of the detectors. The fourth detector had a single (low) discrimination level. For the study of cut-off effects we shall use only the lower level discriminator rates, which will be considered due to protons. Any alphas contributing to this rate would have even lower rigidities (35-43 MV) than the lowest energy protons (~ 50 MV), as evidenced by the lower rates of the high level discriminators which respond only to alphas with > 43 MV rigidity. The electron

energy losses, which are well below the low level thresholds, are indicated in Table III (assuming no large angle scattering). This insensitivity to electrons was verified by other electron sensitive detectors on the same vehicle (Mann, Bloom, and West, 1962, and Seward and Kornblum, 1963).

The geometrical factor $A\Omega(E)$ associated with the three rates is energy dependent, because the wide acceptance angle allows considerable variation in the path length of protons in the detector depletion region. The calculated geometrical factors are shown in Figure 4 as a function of proton energy. The horizontal geometrical factors have been corrected for the absence of protons moving up the line of force with pitch angles less than 70° (such particles would have mirrored below 100 km and been absorbed in the atmosphere).

The count rate R of a detector in a flux $dJ/dE = kE^{-n}$ is given by

$$1) \quad R = \int_0^{\infty} kE^{-n} A\Omega(E) dE$$

The ratios of count rates predicted by Eq. 1 for the three low level discriminators were calculated as a function of the spectral index n . Observed ratios of rates could then be used to determine the actual spectral index.

A small chip of uranium oxide was placed on each detector to provide a low rate alpha-particle continuum for in-flight checks. The rate observed in the equatorial region, consisting of this alpha contamination and secondary particles, was essentially constant during the entire flight for all the discriminator thresholds, verifying the stability of the instrument.

The experiment was launched on 17 September 1961 on Discoverer 31.

Pertinent orbital information is listed in Table IV.

COORDINATE SYSTEM

The coordinate system is chosen to correlate observation with theoretical models of the geomagnetic cavity field. In most models, a dipole moment M is placed perpendicularly to the impinging solar wind, and dipole latitude, local time, and radial distance are used as coordinates. The geographic coordinates θ and ϕ are therefore converted to equivalent dipole latitude and dipole local time DLT, as outlined below.

To state clearly the arguments in the following section, various conventions must be defined distinctly. All parameters associated with a dipole field have the subscript D (e.g., the minimum B-value on a dipole line of force is B_{oD}). All parameters associated with the geomagnetic field have no special subscripts (e.g., B_o); this field includes all the significant terms of the internal field (Finch and Leaton, 1957, Jensen and Whitaker, 1960, Jensen and Cain, 1962). All parameters associated with the geomagnetic cavity field have subscripts GC (e.g., B_{oGC}); this field includes the above geomagnetic field plus the external contributions (Mead, 1963) due to the distortion of the geomagnetic field by the solar wind.

Consider first the definition of the "equivalent dipole latitude" Λ . In a dipole field, the dipole latitude λ of the foot of a line of force is related to the minimum B-value B_{oD} on that line by $\lambda = \cos^{-1} (M/B_{oD})^{1/6}$. By analogy, we define the equivalent dipole latitude Λ of a geomagnetic line of force with a minimum B-value of B_o as

$$2) \quad \Lambda = \cos^{-1} (M/B_o)^{1/6}$$

A more precise justification of Eq. 2 is possible. Midgely and Davis(1963) show that in the dipole cavity field the magnetic field intensity inside $\sim 0.5 R_b$ (R_b is the radial distance of the subsolar point of the boundary) is essentially that of a dipole. Since $R_{bGC} = 8$ to $14 R_e$ (Cahill and Amazeen, 1963), inside 4 to $7 R_e$ in the geomagnetic cavity field the field intensity is essentially that of the geomagnetic field. In this inner region the segments of the geomagnetic lines of force are practically unaffected by the solar wind, and the segments outside are distorted in varying degrees. However, a segment of a geomagnetic line of force beyond $4 R_e$ with a minimum B-value B_o is almost identical to a segment of a dipole line of force with $B_{oD} = B_o$. Thus the theoretical distortion in the dipole cavity field, in which all lines of force with the same B_{oD} undergo the same distortion at a given local time, describes the distortion of the lines with $B_o = B_{oD}$ in the geomagnetic cavity field. Rather than use B_o directly as a coordinate, it is more convenient to use the equivalent dipole latitude as defined in Eq. 2.

In the geomagnetic field, this definition of equivalent dipole latitude is almost the same as the definition of invariant latitude first suggested by O'Brien, Laughlin, Van Allen, and Frank (1962) in the form $\cos^{-1} (1/L)^{1/2}$, where L is the trapped particle invariant (McIlwain, 1961). There are two reasons for the similarity. First, B_o of a line of force is related to L_o , the L-value for particles mirroring at B_o , by $B_o = ML_o^{-3}$ (Stone, 1963). Second, L is almost constant along a geomagnetic line of force, implying that $L \approx L_o$ and $B_o \approx ML^{-3}$.

In the geomagnetic cavity field, the similarity in the two latitudes is removed by the large azimuthal asymmetry. Since we are interested in untrapped particles, we shall use equivalent dipole latitude as defined by Eq. 2.

The other necessary coordinate is the angle between the magnetic meridian plane and the earth-sun line. As a first approximation, we shall consider the earth's field to be a tilted dipole and label the above angle (when expressed in hours) as dipole local time (DLT). The largest error in comparing measurements at a given dipole local time with theoretical models is not due to the dipole approximation, but rather due to the fact that the theoretical calculations assume that the dipole axis is perpendicular to the earth-sun line. For some observations, the dipole is indeed perpendicular to the earth-sun line. For example, in the case shown in Figure 5, the axis of rotation is perpendicular to the earth-sun line (the observations reported here took place Sept. 18-19, 1961), so that at the universal time of 22.7^{hr} the dipole is perpendicular to the earth-sun line. It can be deduced from this figure that the relationship for the dipole local time DLT (Ψ) in hours for a given dipole longitude Ψ (in degrees) is

$$3) \text{ DLT}(\Psi) = \text{DLT}(0^\circ) + \Psi/15 = \text{UT} + (289.8/15) + \Psi/15$$

where UT = universal time and 289.8° is the geographic longitude of the north magnetic pole. However, the dipole is not always perpendicular to the earth-sun line. Figure 6 shows the situation at UT = 13.7 hr. For the line of force illustrated, Eq. 3 would yield DLT = 18 hr, although the plane of the line of force is not perpendicular to the earth-sun line. However, most theoretical models have neglected

the non-perpendicularity of the dipole, and we will do the same in using Eq. 3.

Spreiter and Briggs (1962) performed an exact solution of the approximate boundary condition (Beard, 1960) in the case of a non-perpendicular dipole. Only a small shift in the latitude of the neutral point occurs, and the shape of the boundary (with respect to the earth-sun line) is generally similar to the perpendicular case. In addition, the present data indicate that the cut-off latitude is more strongly dependent on DLT than on the angle the dipole makes with the earth-sun line.

The third coordinate, radial distance, is unnecessary because the data show no significant altitude dependence.

Several orbits are plotted in Λ -DLT space in Figure 7. Usually the northern passes are on the morning side and the southern passes on the evening side, but the two interchange during orbits 9-11 and 25-27, allowing data to be compared at two altitudes at the same Λ and DLT. Also, note that passes 24S and 24N come very close to $\Lambda = 90^\circ$.

RESULTS

Before presenting the cut-off observations, we should discuss details relevant to the interpretation of the cut-off data. First, the observed polar cap flux levels and their time variation are briefly noted. Spectral information is introduced to the extent necessary to identify the vertical fluxes as predominantly 1.5 MeV protons. These fluxes are shown to be far below the level at which collective motion is significant. Finally, related Explorer XII particle and magnetic observations are discussed. We then proceed to show two examples of the observed polar cap count rate which demonstrate these key results: the constant count rate plateau was

observed up to the pole, the darkside cut-off latitude for 1.5 MeV protons was 65° and sharply defined, the sunside cut-off latitude was 67° and very diffuse, and the cut-off latitudes for horizontal and vertical directions were nearly identical. These results are further emphasized by the consistency of the cut-off latitudes observed on all available polar passes over both polar regions.

The vertical flux of protons with 1.5 - 4.4 MeV is shown in Fig. 8a as a function of polar pass and universal time. Only the northern passes are plotted since the southern passes are quite similar. The range of flux levels observed in the count rate plateau region on each pass is indicated by the length of the vertical bars. These variations are not significant in the present study.

Figure 8b indicates the spectral index γ , which is derived as previously mentioned. The value of -2 to -3 for γ is quite similar to the "harder" solar events reported by Pieper, et. al., (1962). Since the ratio of counts in the 1.5 - 4.4 MeV interval to counts in the 6 - 8 MeV interval is between 20 and 60, most of the observed flux must have been 1.5 MeV protons and not 4.4 MeV protons. Thus, the lowest observed flux level of $\sim 4 \text{ cm}^{-2} \text{ sec}^{-1}$ and the maximum flux of $\sim 40 \text{ cm}^{-2} \text{ sec}^{-1}$ are mostly 1.5 MeV protons. Both fluxes are well below the critical flux level at which collective motion occurs in the geomagnetic field.

Obayashi and Hakuru (1961), following Ferraro (1952), have noted that individual particle motion is dominant when the plasma shielding distance is larger than the geomagnetic field impact parameter (the Störmer unit). For 1.5 MeV protons, the critical flux is $\sim 200 \text{ cm}^{-2} \text{ sec}^{-1}$. Although separation of individual and collective particle motion is not a sharp one, the 1.5 MeV fluxes reported here are sufficiently low to insure individual particle motion. Previous non-storm measurements (Table II) were

of much larger flux levels with the consequent possibility that collective motion was of importance.

The precise extraterrestrial origin of these protons is not clear. The low proton flux of $\sim 0.1 \text{ cm}^{-2} \text{ sec}^{-1} \text{ sr}^{-1} \text{ MeV}^{-1}$ observed in early orbits is possibly the trail of low energy protons detected by the Explorer XII satellite (McDonald, private communication) following the 10 September 1961 flare. The increase at ~ 1200 UT on 18 Sept. 1961 was also detected by Explorer XII (Bryant, et. al., 1963), and was of similar flux level and spectral shape as reported here (U. D. Desai, private communication). Bryant, et. al., (1963) speculate that this event is similar to two other long-lived recurrent solar events which they have observed.

Finally, details of the state of the magnetic field are important. Explorer XII magnetometer data (Cahill and Amarn, 1963) locate the magnetospheric boundary at $> 13.5 R_e$ on September 18, 1961, and at $12 R_e$ on 19 September 1961 (in each case at 10 hr local time). The field inside was regular (Cahill, private communication). The absence of unusual compression and of storm-time ring currents is also supported by ground based measurements (Lincoln, 1962, a, b, c), which indicate that no magnetic storms occurred between 15 September 1961 and 23 September 1961. The absence of large magnetic disturbances is also evident from the K_p index (Figure 8d, from Solar-Geophysical Data, Part B, CRPL), especially on 19 September 1961, which was one of the five quietest days that month.

In summary, the following details are important to further discussion. First, there is evidence that during this time the magnetic field was not unusually disturbed or compressed, and in particular, there is no evidence of a storm-time ring current. Second, the same proton flux and spectrum was observed near the equatorial

plane beyond $10 R_e$. Third, the lowest proton flux level observed is well below the critical flux which separates individual and collective particle motion in the geomagnetic field. Fourth, the vertical fluxes reported here are predominantly 1.5 MeV protons.

We now proceed to the description of the cut-off latitudes observed under the above circumstances. The vertical (1.5 - 4.4 MeV) and horizontal (1.1 - 6 MeV) proton fluxes during successive southern and northern passes are shown in Figure 9. These particular passes are displayed because the vehicle passes almost directly over $\Lambda = 90^\circ$ (c.f. Figure 7). The presence of the proton flux over the entire range of latitudes argues against a trapped-particle origin. Figure 9 also shows that the horizontal proton flux is $\sim 40\%$ higher than the vertical proton flux, a factor which is consistent with an $E^{-2.5}$ spectrum with a correction to the horizontal geometrical factor to account for allowed pitch angles. The final feature of Figure 9 is the abrupt transition between equatorial background and the polar proton fluxes. Note that the darkside transition is more abrupt and at a lower latitude than the sunside transition, and that the horizontal and vertical cut-off latitudes are quite similar.

In order to further discuss the cut-off transition, two definitions must be employed to cope with the statistical variation associated with such low count rates (0.1 to 2 sec^{-1}). The foot of the polar region is defined as the equivalent dipole latitude of the satellite when the waiting times (c.f. Evans, 1955) between observed events are so short that the probability is less than 5% that they belong to the equatorial rate. Thus, the latitude of the polar foot is a measure of the position where extraterrestrial particles are first detectable. In a similar fashion, the knee of the

polar plateau region is the equivalent dipole latitude of the satellite when the waiting times are so long that the probability is less than 5% that they belong to the polar rate. Thus the latitude of the polar knee is a measure of the extent of the polar plateau, and the difference $\Delta\Lambda$ between knee and foot is a measure of the width of the cut-off transition. Typical critical waiting times τ_c which are appropriate to the above definitions are listed in Table V. Note that when the polar count rate is less than 0.4 sec^{-1} ($\text{flux} < 0.4 \text{ cm}^{-2} \text{ sec}^{-1} \text{ sr}^{-1} \text{ MeV}^{-1}$), $\Delta\Lambda$ cannot be meaningfully measured. In general, the error in the determination of the foot is of the order of τ_c , during which time the satellite traverses $\sim 1^\circ$ in latitude. A comparable error results from the timing information.

The polar foot and knee latitudes for vertically incident 1.5 MeV protons are shown for all available passes in Figures 10 and 11. The darkside data (Figure 10) for northern and southern passes are grouped together, even though they occur at different dipole local times. The consistent fit would suggest no dependence on dipole local time (DLT) between DLT = 2100 and 0400. A systematic universal time variation does appear in orbits 13 - 15, (1600 - 2000 UT, 18 September 1961), but no correlating magnetic data has been found. Figure 10 also shows the angle of the eccentric dipole axis with respect to the earth-sun line. No systematic dependence is seen.

The northern and southern sunside passes (Figure 11) are not grouped together because of the significant dipole local time dependence. Again, no systematic dependence of foot or knee latitude on θ_{DS} is noted. A complex time dependence is apparent, since the polar knee latitude is higher in orbits 23 - 29, while the polar foot latitude is relatively unchanged. Note that the darkside data (Figure 10)

show no similar variation, suggesting that the polar foot latitude is somewhat stable, while the transition width at local noon is subject to considerable variation.

Since the dominant variation in Figures 10 and 11 is dependent on dipole local time, the polar knee and foot latitudes (for vertical 1.5 MeV protons) are plotted versus dipole local time (Figures 12 and 13). The northern and southern passes are indicated in order to illustrate that the data from both regions are remarkably consistent when displayed in this coordinate system. The most interesting and striking feature is that the polar foot latitude is $2 - 3^\circ$ higher on the dayside than on the nightside, and that the knee latitude shows an asymmetry of more than 5° . As discussed later, the higher latitude at local noon compared to local midnight is qualitatively expected from the asymmetrical distortion of the magnetosphere by the solar wind, but an exact explanation is more difficult.

The dipole local time dependence of the transition width has already been noted. Figure 14 shows this dependence explicitly (passes before 0900, 18 Sept. 1961, are not included because the rate was too low to determine $\Delta\Lambda$). Excluding 0900 to 1500 DLT, the value for $\Delta\Lambda$ is $0.9 \pm 0.6^\circ$. Between 0900 and 1500 DLT, there is much time variation, and in general the transition is several times wider.

DISCUSSION

We first discuss the present observations as compared to earlier polar cap blackout, polar cap absorption, and 1 - 15 MeV proton flux measurements. The importance of the present results to the interpretation of these earlier measurements is examined, followed by a discussion of the severe test which the present observations pose for various cut-off models, none of which appear to be

immediately applicable. Finally, a qualitative explanation of the higher local noon cut-off latitude is discussed.

It is likely that the observed cut-off effects are of the same nature as cut-offs noted by study of polar cap blackout (Bailey, 1959, Obayashi and Hakuru, 1960), polar cap absorption (Reid and Collins, 1959, Reid and Leinbach, 1959, Axford and Reid, 1962 and 1963), and the 1 - 15 MeV fluxes reported by Pieper, et. al. (1962) and Zmuda, et. al. (1963). The latter two directly measured proton fluxes on Injun I, but neither sharply defined the energy nor demonstrated the local time dependence of the cut-off latitude. The other measurements all show cut-off latitudes of $\Lambda = 65^\circ - 70^\circ$, but could specify neither flux and energy nor determine the local time dependence. All of the above measurements were of proton flux levels $\gtrsim 300 \text{ cm}^{-2} \text{ sec}^{-1}$.

The present measurement of a very low cut-off latitude for 1.5 MeV protons poses a severe problem for presently postulated models which have been able to account for the previous observations. In the case of polar cap blackout and radio noise absorption, the exact energy was not known, so no severe discrepancy was apparent. In fact, it was often assumed that a polar knee latitude of $\Lambda = 65^\circ - 70^\circ$ indicated that protons with $\sim 10 \text{ MeV}$ (i.e., with Störmer cut-off $\Lambda = 72^\circ$) were not present (i.e., the solar flare spectrum was cut off, c.f. Reid, 1961) or that the solar flare spectrum is exponential in character (Webber, 1962). [Note that other evidence is available supporting an exponential rigidity spectrum for $E > 70 \text{ MeV}$ (Freier and Webber, 1963).] The present observation of a polar cap which is open down to 65° for all protons with $E \approx 1.5 \text{ MeV}$ suggests that the fluxes and spectra responsible for polar cap ionization be re-evaluated.

In the case of previous direct measurements of protons on Injun I the energy interval (1 - 15 MeV) was considerably wider than in the present case, and no second interval at low energies (such as 6 - 8 MeV) was available to sharply define the spectrum. In addition, all of the data reported for the July 1961 events were collected at local noon, where the polar knee latitude may be 70° at the same time it is 65° on the darkside. The combination of high latitude (70°) and broad energy interval (1 - 15 MeV, with Störmer cut-offs of 71° - 77°) did not pose such a severe problem for cut-off models, although Akasofu and Lin (1963) could show that a simple ring current model was not adequate.

The present observation provides a severe test for other cut-off models. The model proposed by Akasofu, et. al. (1963) depends on the two neutral points characteristic of the boundary of the geomagnetic field in a field-free, cold solar wind. Low rigidity (0.5 MeV) protons gain access to the geomagnetic field at the two neutral points and are guided along the lines of force connecting the neutral points to the ionosphere. Aside from the considerable range of latitudes predicted by various calculations for the feet of these lines (compare Akasofu, 1963, Spreiter and Briggs, 1961, and Midgley and Davis, 1963), all calculations place these lines at local noon, making it difficult for this model to explain the cut-off latitude on darkside.

The cut-off model described by Obayashi and Hakuru (1961) depends on the superposition of a uniform field anti-parallel to the dipole field to achieve very low cut-off latitudes. However, the anti-parallel field is suggested for the main phase of magnetic storms. In absence of a main phase, the nearly uniform field due to the pressure of the solar wind is parallel to the dipole, and an increase

in cut-off latitude (as compared to Störmer cut-off) is predicted, which is not in agreement with the present observations.

Another model of the magnetosphere depends on the presence of an interplanetary magnetic field with a generally southerly direction in the vicinity of the Earth (Dungey, 1962). It is suggested that the auroral zone ($\sim 65^\circ$) divides those lines of force with both feet on the Earth ($< 65^\circ$) and those lines connected to the interplanetary field, and consequently with only one foot attached to the Earth. A probable consequence would be an abrupt decrease in cut-off rigidity above 65° (see Reid and Leinbach, 1959, for a similar suggestion of linking high latitude lines of force to the interplanetary field). However, the observation of the magnetospheric boundary at $> 12 R_e$ at the time of the measurements reported here would indicate that no lines up to at least 73° latitude were connected to the interplanetary field at the time of observation. Thus, this model would also require a more detailed examination in order to describe the observations.

One other possibility is suggested by the observed cut-off latitude of 65° . Axford and Hines (1961) postulate that the outer magnetosphere is convecting under the influence of a viscous-like interaction between the solar wind and the surface of the magnetosphere. They suggest that if the magnetospheric boundary is at $8 R_e$ and if the lines of force above 62° are connecting, the observed local time dependence of the latitude of maximum incidence of auroral displays, geomagnetic agitation and bay disturbances is a natural consequence. An increase in the latitude of the edge of the convecting region to $\sim 65^\circ$ during less disturbed conditions might be expected from the 2° to 3° shift in the median auroral latitude as a function of K_p (Gartlein and Sprague, 1962). However, the effect of the

relatively slow magnetospheric convection on protons with velocities of the order of 10^9 cm sec^{-1} is open to question.

Although none of the above models seem to predict a cut-off latitude of 65° for 1.5 MeV protons, a qualitative explanation of the higher latitude during local day relative to local night can be found by considering the cut-off model proposed by Ray (1963) specifically for near-dipole fields with slight azimuthal asymmetry, e.g., the geomagnetic field in absence of any external current systems. In such fields, the particle invariant L is nearly constant for all particles on a line of force, implying that $L \approx L_0 \equiv (M/B_0)^{1/3}$ (Stone, 1963). Ray points out that when $L \approx L_0$, the cut-off rigidity R in the direction along the line of force is

$$R(BV) = 14.9/L^2 = 14.9 (B_0/M)^{2/3}$$

Thus, lines of force in the geomagnetic field with the same B_0 have the same cut-off. The geomagnetic cavity field, however, is highly asymmetric, and Ray makes no attempt to extend the above result to this field. Nevertheless, the configuration of lines of force with the same B_{0GC} in the geomagnetic cavity field ~~do~~^g give a qualitative suggestion as to the relative cut-off latitudes at local noon and midnight.

For this purpose it is not necessary to determine the exact configuration of the lines; it is sufficient to recognize that the compression of the field is larger on the sunside than on the darkside, which means that a line of force at a given equivalent dipole latitude (i.e., with a given B_0 without external field, as indicated in Eq. 2) will have a larger B -value (B_{0GC}) in the geomagnetic cavity field, and

that B_{oGC} will be largest when the field is most compressed (i.e., at local noon). Thus, it is necessary to go to a higher latitude line at local noon than at local midnight to obtain the same B_{oGC} , and qualitatively it might be expected that the same rigidity cut-off occurs at higher latitudes at local noon than at local midnight. This is indeed the observed case. It should be pointed out, however, that though this simple consideration yields the correct sign of the local time dependence of the cut-off latitude, it does not yield correct numerical values. Using Mead's (1963) expansion of the cavity field with $R_b = 12 R_e$, it is found that a line of force at $\sim 65.7^\circ$ at local noon has the same B_{oGC} as the line at 65° at local midnight. The observed asymmetry is $\sim 2^\circ$ for the foot, and $\sim 5^\circ$ for the knee.

SUMMARY

The above results can be described specifically as a unique observation of a very small polar flux of 1.5 MeV protons, interacting as individual particles with the geomagnetic cavity field. The flux ^{was} isotropic over the upper hemisphere. During this time, the magnetic field was not unusually disturbed; the magnetospheric boundary was beyond $12 R_e$ on the day side. However, the vertical cut-off latitude on the nightside was $\Lambda = 65^\circ$, as compared to a Störmer cut-off of 76° . The nightside transition width was $\sim 1^\circ$. On the dayside, the cut-off was at $\sim 67^\circ$, and the transition width was $\sim 3^\circ$ and variable. The horizontal cut-off latitudes were similar. These results indicate that the entire polar cap region is accessible to 1.5 MeV protons. This feature of the geomagnetic cavity field presents a severe problem for present cut-off models. Such a low cut-off latitude in absence of a magnetic storm also suggests the re-examination of the calculations of the proton

fluxes associated with pre-SC polar cap blackout and polar cap absorption.

ACKNOWLEDGMENTS

Special thanks are extended to my faculty sponsor, Dr. J. A. Simpson, and to Dr. C. Y. Fan, who most generously offered their unanalyzed data from Discoverer 31 when a later satellite experiment yielded too little data for a thesis. Drs. Fan and Simpson were ably assisted in the design and fabrication of the flight package by J. E. Lamport, L. Petraitis, R. Takaki, A. Tuzzolino, M. Perkins, H. Thomas, J. Stepney, and H. Tibbs of the Laboratory for Applied Sciences of the University of Chicago. The analysis of the data was greatly facilitated by the efforts of C. M. Case, G. Lentz, R. Taft, A. Krauss, and T. H. Chang.

This experiment was launched on Discoverer 31 under the auspices of the Geophysical Research Directorate, Air Force Cambridge, through the efforts of Dr. L. Katz and Mr. L. Letteman. Dr. F. Seward of Lawrence Radiation Laboratory (LRL) kindly provided the timing parameters necessary for reducing the tape recorded data. Without this timing information the present investigation would have been much more difficult, if not impossible. Channels on the flight tape recorder were available to us through the generosity of the LRL group.

I am most grateful to Drs. F. B. McDonald, U. D. Desai, and L. J. Cahill for the communication of their 18-19 September 1961 observations prior to publication, and to Dr. E. N. Parker for his helpful discussion. Dr. K. Kondo not only provided valuable comments, but also made available the computer programs used for tracing lines of force in the geomagnetic cavity field.

- Akasofu, S. I., Deformation of magnetic shells during magnetic storms, J. Geophys. Res., 68, 4437-45, 1963.
- Akasofu, S. I., and W. C. Lin, The magnetic moment of model ring current belts and the cut-off rigidity of solar protons, J. Geophys. Res., 68, 973-977, 1963.
- Akasofu, S. I., W. C. Lin, and J. A. Van Allen, The anomalous entry of low-rigidity solar cosmic rays into the geomagnetic field, J. Geophys. Res., 68, 5327 - 5338, 1963.
- Axford, W. I., and C. O. Hines, A unifying theory of high-latitude geophysical phenomena and geomagnetic storms, Can. J. Phys., 39, 1433-1464, 1961.
- Axford, W. I., and G. C. Reid, Polar-cap absorption and the magnetic storm of February 11, 1958, J. Geophys. Res., 67, 1692-1696, 1962.
- Axford, W. I., and G. C. Reid, Increases in intensity of solar cosmic rays before sudden commencements of geomagnetic storms, J. Geophys. Res., 68, 1793 - 1803, 1963.
- Bailey, D. K., Abnormal ionization in the lower ionosphere associated with cosmic-ray flux enhancements, Proc. IRE, 47, 255-266, 1959.
- Beard, D. B., The interaction of the terrestrial magnetic field with the solar corpuscular radiation, J. Geophys. Res., 65, 3559-3568, 1960.
- Bryant, D. A., T. L. Cline, U. D. Desai, and F. B. McDonald, New evidence for long-lived solar streams in interplanetary space, Phys. Rev. Letters, 11, 144-146, 1963.
- Cahill, L. J., and P. G. Amazeen, The boundary of the geomagnetic field, J. Geophys. Res., 68, 1835-1843, 1963.

Dungey, J. W., The interplanetary field and auroral theory, J. Phys. Soc. Japan, 17, Supplement A-II, 15-19, 1962.

Evans, R. D., The Atomic Nucleus, McGraw Hill Book Co., Inc., New York, 1955.

Fan, C. Y., J. A. Simpson, and E. C. Stone, The magnetospheric cut-off for 1.5 MeV extra-terrestrial protons, submitted to Phys. Rev. Letters, 1964.

Ferraro, V. C. A., On the theory of the first phase of a geomagnetic storm: A new illustrative calculation based on an idealized (plane not cylindrical) model field distribution, J. Geophys. Res., 57, 15-49, 1952.

Finch, H. F., and B. R. Leaton, The earth's main magnetic field - Epoch 1955.0, Monthly Notices Roy. Astron. Soc., Geophys. Suppl. 7, 314-317, 1957.

Freier, P. S., and W. R. Webber, Exponential rigidity spectrums for solar flare cosmic rays, J. Geophys. Res., 68, 1605-1629, 1963.

Gartlein, C. W., and G. Sprague, Auroral absorption of radio signals, J. Geophys. Res., 67, 3393-3396, 1962.

Jensen, D. C., and J. C. Cain, An interim geomagnetic field, Trans. Am. Geophys. Union, 43, 209, 1962.

Jensen, D. C., and W. A. Whitaker, A spherical harmonic analysis of the geomagnetic field, J. Geophys. Res., 65, 2500, 1960.

Lincoln, J. Virginia, Geomagnetic and solar data, J. Geophys. Res., 67, 381-387, 1962a.

Lincoln, J. Virginia, Geomagnetic and solar data, J. Geophys. Res., 67, 2025-2037, 1962b.

Lincoln, J. Virginia, Geomagnetic and solar data, J. Geophys. Res., 67, 4875-4877, 1962c.

- Maehlum, B., and B. J. O'Brien, Solar cosmic rays of July 1961 and their ionospheric effects, J. Geophys. Res., 67, 3269-3279, 1962.
- Mann, L. G., S. D. Bloom, and H. I. West, Jr., The electron spectrum from 90 to 1200 KeV as observed on Discoverer satellites 29 and 31, Lawrence Radiation Lab. Rept. UCRL-6902, 1962.
- McIlwain, C. E., Coordinates for mapping the distribution of geomagnetically trapped particles, J. Geophys. Res., 66, 3681-3692, 1962.
- Mead, G. D., The geomagnetic field near the magneto-pause, Trans. Am. Geophys. Union, 44, 82, 1963.
- Midgely, J. E., and L. Davis, Jr., Calculation by a moment technique of the perturbation of the geomagnetic field by the solar wind, J. Geophys. Res., 68, 5111-5123, 1963.
- Obayashi, T., and Y. Hakuru, Enhanced ionization in the polar ionosphere associated with geomagnetic storms, J. Atmospheric Terrest. Phys., 18, 101-122, 1960.
- Obayashi, T., and Y. Hakuru, Polar ionospheric disturbances and solar corpuscular emissions, Planet. Space Sci., 5, 56-69, 1961.
- O'Brien, B. J., C. D. Laughlin, J. A. Van Allen, and L. A. Frank, Measurements of the intensity and spectrum of electrons at 1000-kilometer altitudes and high latitudes, J. Geophys. Res., 67, 1209-1225, 1962.
- Pieper, G. F., A. J. Zmuda, and C. O. Bostrom, Solar protons and magnetic storms in July 1961, J. Geophys. Res., 67, 4959-4981, 1962.
- Ray, E. C., On the motion of charged particles in the geomagnetic field, Ann. Phys., 24, 1-18, 1963.

Rees, Janice M., and D. G. King-Hele, Table of the artificial earth satellites launched in 1957-62, Planet. Space Sci., 11, 1053-1083, 1963.

Reid, G. C., A study of the enhanced ionization produced by solar protons during a polar cap absorption event, J. Geophys. Res., 66, 4071-4085, 1961.

Reid, G. C., and C. Collins, Observations of abnormal VHF radio wave absorption at medium and high latitudes, J. Atmospheric Terrest. Phys., 14, 63-81, 1959.

Reid, G. C. and H. Leinbach, Low-energy cosmic-ray events associated with solar flares, J. Geophys. Res., 64, 1801-1805, 1959.

Seward, F. D., and H. N. Kornblum, Jr., Near-earth charged-particle backgrounds measured with polar orbiting satellites, Lawrence Radiation Lab. Rept. UCRL-6693, 1963.

Spreiter, J. R., and B. R. Briggs, Theoretical determination of the form of the boundary of the solar corpuscular stream produced by interaction with the magnetic dipole field of the earth, J. Geophys. Res., 67, 37-51, 1962.

Stone, E. C., The Physical significance and application of L , B_0 and R_0 to geomagnetically trapped particles, J. Geophys. Res., 68, 4157-4166, 1963.

Takaki, R., M. Perkins, and A. Tuzzolino, A gold-silicon surface barrier proton range telescope, IRE Trans. on Nuc. Sci., NS-8, 64-72, 1961.

Webber, W. R., The production of free electrons in the ionospheric D layer by solar and galactic cosmic rays and the resultant absorption of radio waves, J. Geophys. Res., 67, 5091-5106, 1962.

Zmuda, A. J., G. F. Pieper, and C. O. Bostrom, Solar protons and magnetic storms in February 1962, J. Geophys. Res., 68, 1160-1165, 1963.

TABLE I

Pre-Sudden Commencement Solar Proton Events; Indirect Measurements

<u>Observer</u>	<u>Date</u>	<u>Observation</u>	Extent (Geomagnetic Latitude)
<u>Bailey (1959)</u>	23 Feb. 1956	Polar Cap Blackout	$> 60^{\circ} - 70^{\circ}$
<u>Reid and Collins (1959)</u>	2 events, 1957	Polar Cap Absorption	$> 67^{\circ}$
<u>Reid and Leinbach (1959)</u>	24 events (May '57 to July, 1959)	Polar Cap Absorption	$> 65^{\circ}$
<u>Obayashi and Hakuru (1960)</u>	13 Sept. 1957	Polar Cap Blackout	$> 60^{\circ} - 65^{\circ}$
<u>Axford and Reid (1962)</u>	11 Feb. 1958	Polar Cap Absorption	$> 64.7^{\circ}$
<u>Axford and Reid (1963)</u>	30 Sept. 1961	Polar Cap Absorption	$65^{\circ} - 70^{\circ}$

Table II

Pre-Sudden Commencement Solar Proton Events;
Direct Measurements of Large Fluxes of 1.5 - 15 MeV Protons

<u>Date</u>	<u>Threshold Latitude</u>	<u>Plateau Latitude</u>	<u>Flux (cm⁻² sec⁻¹ sr⁻¹)</u>
12 July 61*	66.1	74.1	410
13 July 61*	62.9	-	≥ 1500
20 July 61*	63.4 - 65.9	> 72	300
20 July 61*	64.3	-	520
26 July 61*	64.5	71.6	520
26 July 61*	65.0	-	630
29 Sept. 61*	64.7	67.8	-
2 Feb. 62 ⁺	65	-	-
4 Feb. 62 ⁺	65.7	-	-

* Pieper, et. al., 1962

⁺Zmuda, et. al., 1963

TABLE III

Typical Detector Characteristics

AuSi Surface Barrier

Total Thickness	48 mg-cm^{-2}
Resistivity	$1450 \ \Omega \text{-cm}$
Applied Bias	6.5 V
Depletion Thickness	12 mg-cm^{-2}
Diameter	0.38 cm
Energy Loss Threshold	> 830 keV
Energy Loss: Relativistic electron (Perpendicular Incidence)	20 keV
Maximum Electron Energy Loss (Perpendicular Incidence)	100 keV
Alpha Contamination Rate	0.025 sec^{-1}
Mylar Light Shield (Aluminized)	0.22 mg-cm^{-2}

TABLE IV*

Discoverer 31, 1961 $\alpha\beta$

Launch	17 September 1961 at 2107 UT
Orbital Inclination	82.70°
Nodal Period	90.86 min
Perigee Height	235 km
Apogee Height	396 km
Perigee Latitude	43° N on sunside

* (Rees and King-Hele, 1962)

TABLE V

Critical Waiting Times

	τ_c
Polar Foot, Vertical (1.5 - 4.4 MeV)	15 sec
Polar Foot, Horizontal (1.1 - 6 MeV)	13 sec
Polar Knee, where $dJ/dE \sim 0.1 \text{ cm}^{-2} \text{ sec}^{-1} \text{ sr}^{-1} \text{ MeV}^{-1}$	30 sec
Polar Knee, for $dJ/dE \sim 0.4 \text{ cm}^{-2} \text{ sec}^{-1} \text{ sr}^{-1} \text{ MeV}^{-1}$	11 sec
Polar Knee, for $dJ/dE \sim 1 \text{ cm}^{-2} \text{ sec}^{-1} \text{ sr}^{-1} \text{ MeV}^{-1}$	5 sec

FIGURE CAPTIONS

- Fig. 1. Cross section view of the arrangement of the two circular detectors and the circular aperture of the aluminum collimator which make up each telescope.
- Fig. 2. Schematic representation of the orientation and view angles of the detector telescopes. The vehicle velocity vector is directed out of the page. The experiment was mounted in space provided by Air Force Cambridge (GRD).
- Fig. 3. Calculated energy loss in the 12 mg-cm^{-2} depletion depth of AuSi detectors as a function of incident energy for the front and rear detectors in a counter telescope. The electronic thresholds on the various detectors are indicated. The calculation assumes perpendicular incidence.
- Fig. 4. Calculated geometrical factors associated with the low level discriminator rates as a function of incident proton energy. The horizontal geometrical factors are corrected for allowed pitch angles (α) as noted in text.
- Fig. 5. Schematic representation of the orientation of a line of force with respect to the earth-sun line at 22.7 hr UT at equinox. M is the dipole field, tilted $\sim 11.5^\circ$ to the axis of rotation of the earth. ϕ is geographic longitude. ψ is dipole longitude.
- Fig. 6. Schematic representation of a tilted dipole line of force for 13.7 hr UT, showing the effect of the tilt of the dipole on the orientation of a magnetic field line with respect to the earth-sun direction. ϕ is geographic longitude. ψ is dipole longitude.
- Fig. 7. Typical vehicle trajectories plotted as a function of equivalent dipole latitude Λ and dipole local time. The label 17N indicates the 17th

northern pass. The direction of the satellite along the trajectory is also shown.

Fig. 8. a) The vertically incident proton flux (1.5 - 4.4 MeV) as a function of polar pass number.

b) The spectral index n in $dJ/dE = kE^{-n}$.

c) The count rate observed by the 1.4 - 4.4 MeV vertical detector in the equatorial regions. The counts are from alpha contamination and secondaries.

d) The magnetic field disturbance as indicated by the K_p index.

Fig. 9. Count rates observed on two successive southern and northern passes, showing that the plateau flux extends to the pole and that the darkside transition at $\Lambda = 65^\circ$ is at a lower latitude and is more abrupt than the sunside transition. ∇ indicates the vertical (1.5 MeV proton) flux; H indicates the horizontal proton flux. Statistical error: $\pm 12\%$.

Fig. 10. The latitude Λ of the nightside polar foot and knee for vertical and horizontal fluxes. Note that northern and southern passes are consistent, even though they occur at different dipole local times (DLT). The angle θ_{DS} of the eccentric dipole with respect to the earth-sun line is also shown.

Fig. 11. The latitude Λ of the dayside polar knee and foot for vertical (1.5 MeV proton) and horizontal proton fluxes. The northern and southern passes are plotted separately because of the large dipole local time (DLT) dependence. No systematic dependence on the angle θ_{DS} between the dipole and the earth-sun line is noted.

Fig. 12. The location of the polar foot for vertically incident 1.5 MeV protons as observed on all available orbits. The coordinate system is equivalent dipole latitude Λ and dipole local time. Note that the latitude of the polar foot is $\sim 2^\circ$ higher at local noon than at local midnight.

Fig. 13. The location of the polar knee for vertically incident 1.5 MeV protons in dipole equivalent latitude and dipole local time coordinates. Note that the knee latitude is $\sim 70^\circ$ at local noon and $\sim 65^\circ$ at midnight.

Fig. 14. The vertical transition width $\Delta\Lambda$ (knee latitude minus foot latitude) for 1.5 MeV protons as a function of dipole local time. Only data from orbits 8 through 30 (ϕ 8 through ϕ 30) is included, as noted in text.

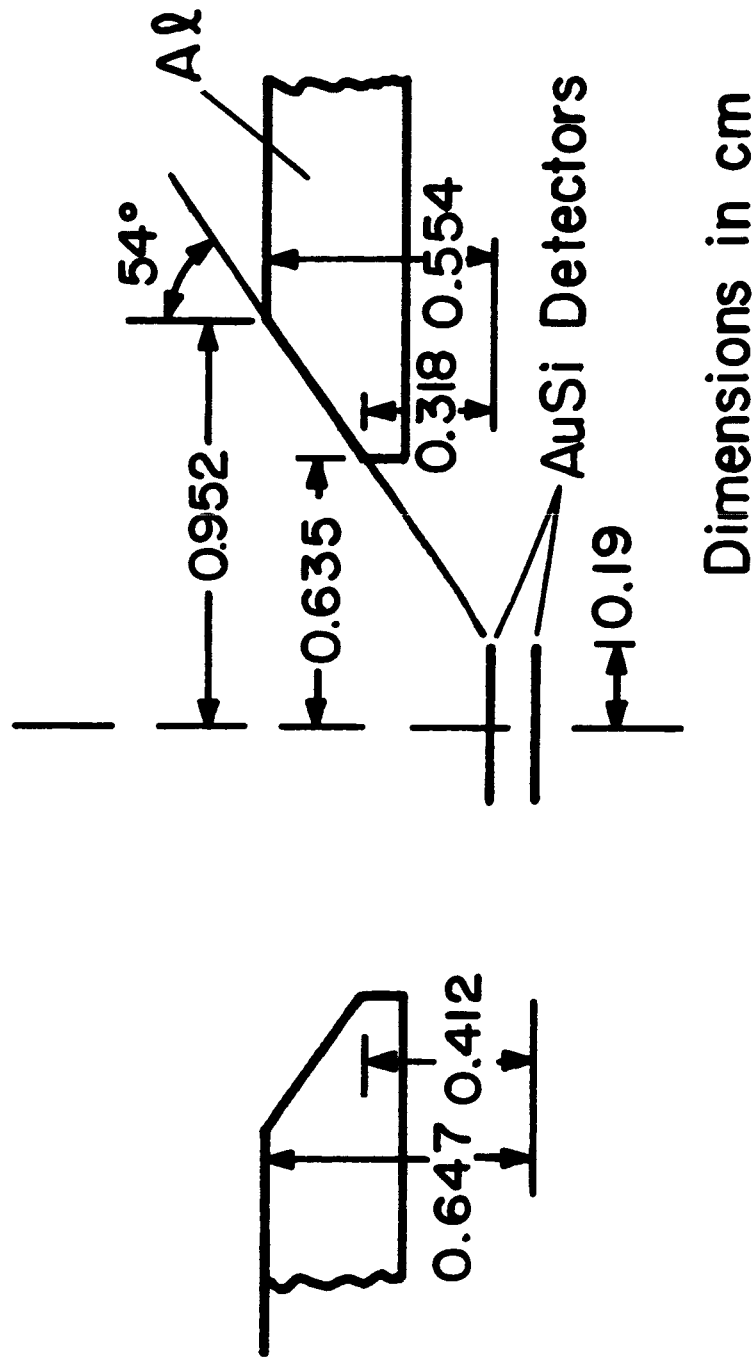


Fig.1

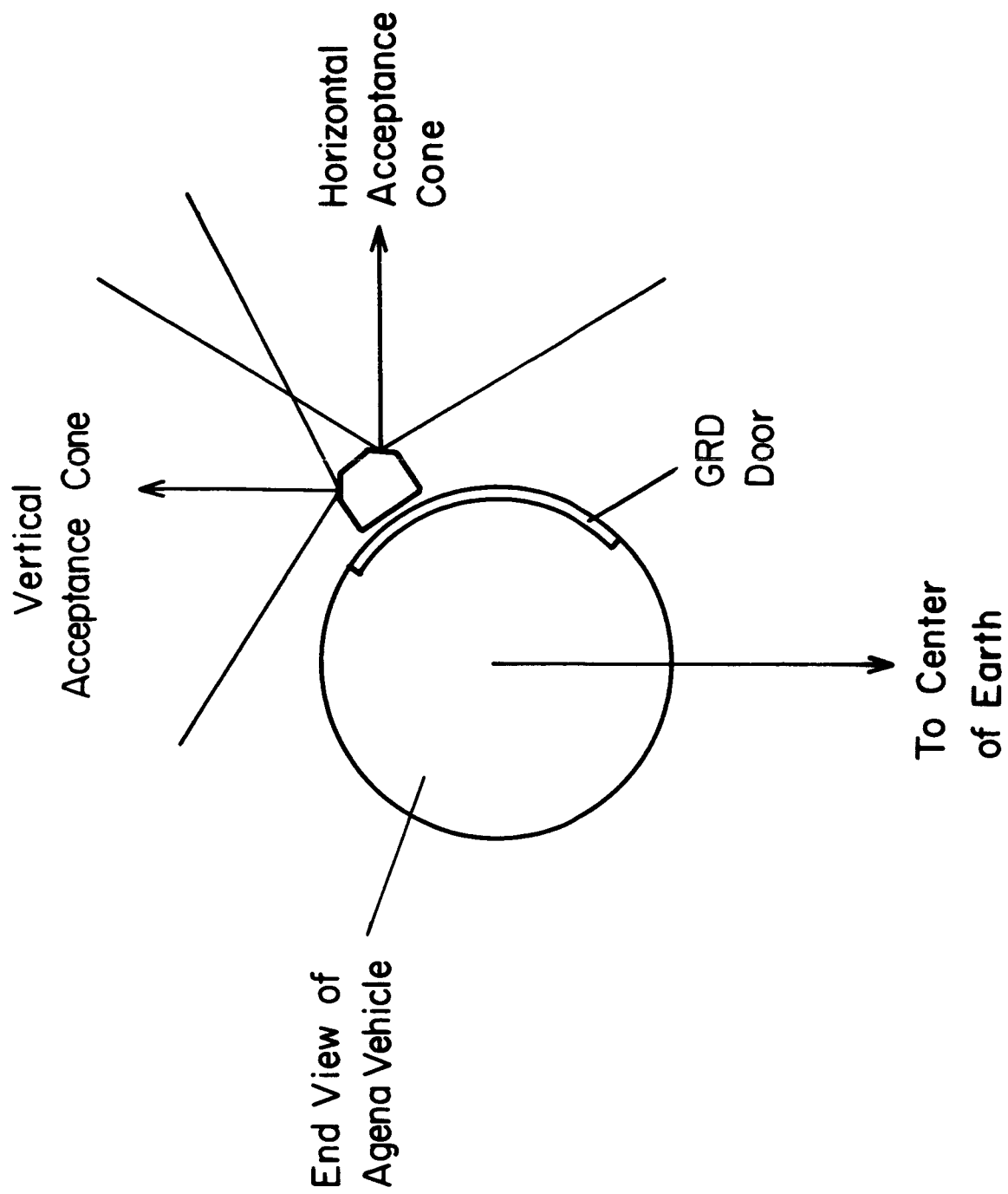


Fig. 2

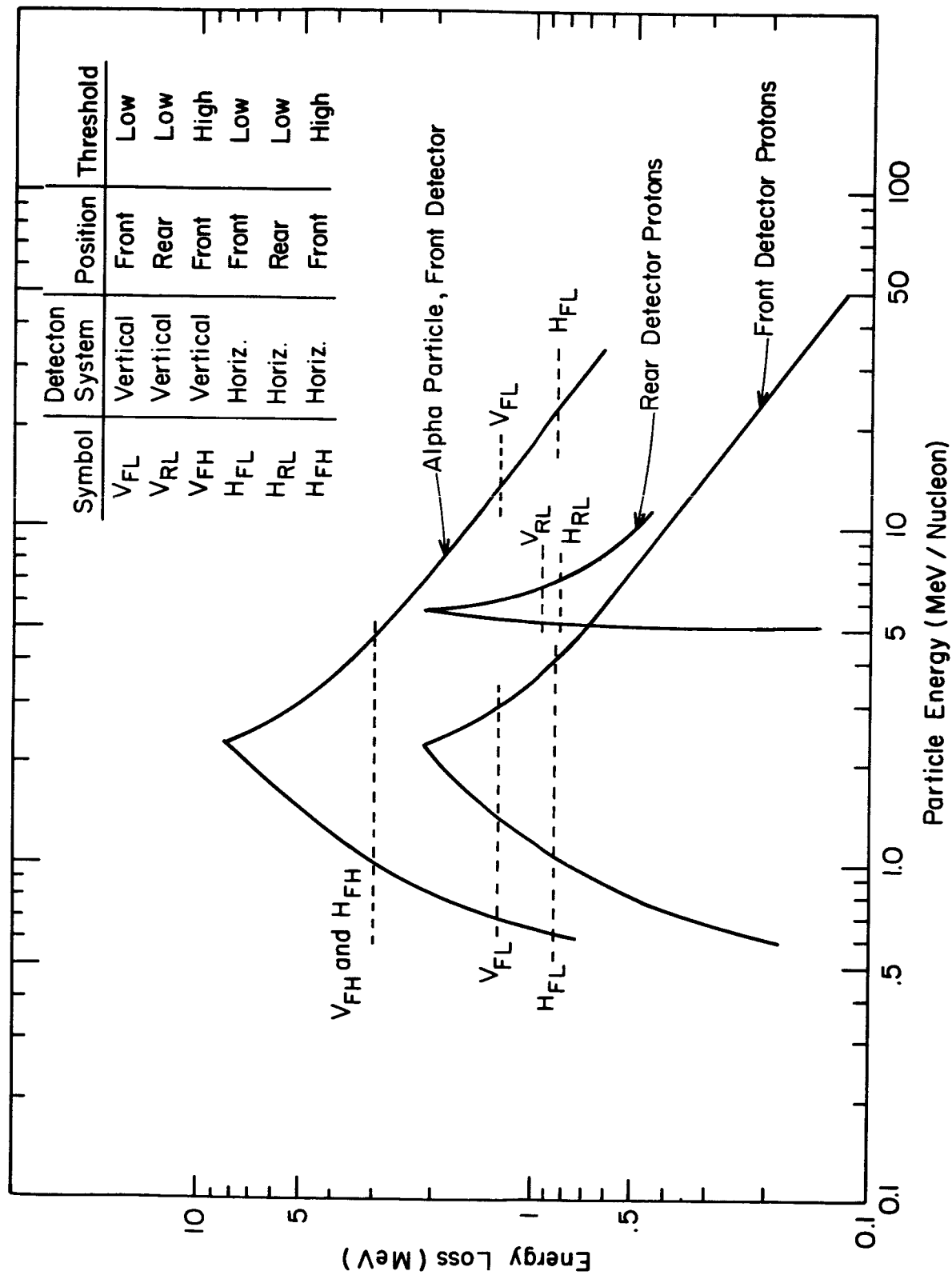


Fig. 3

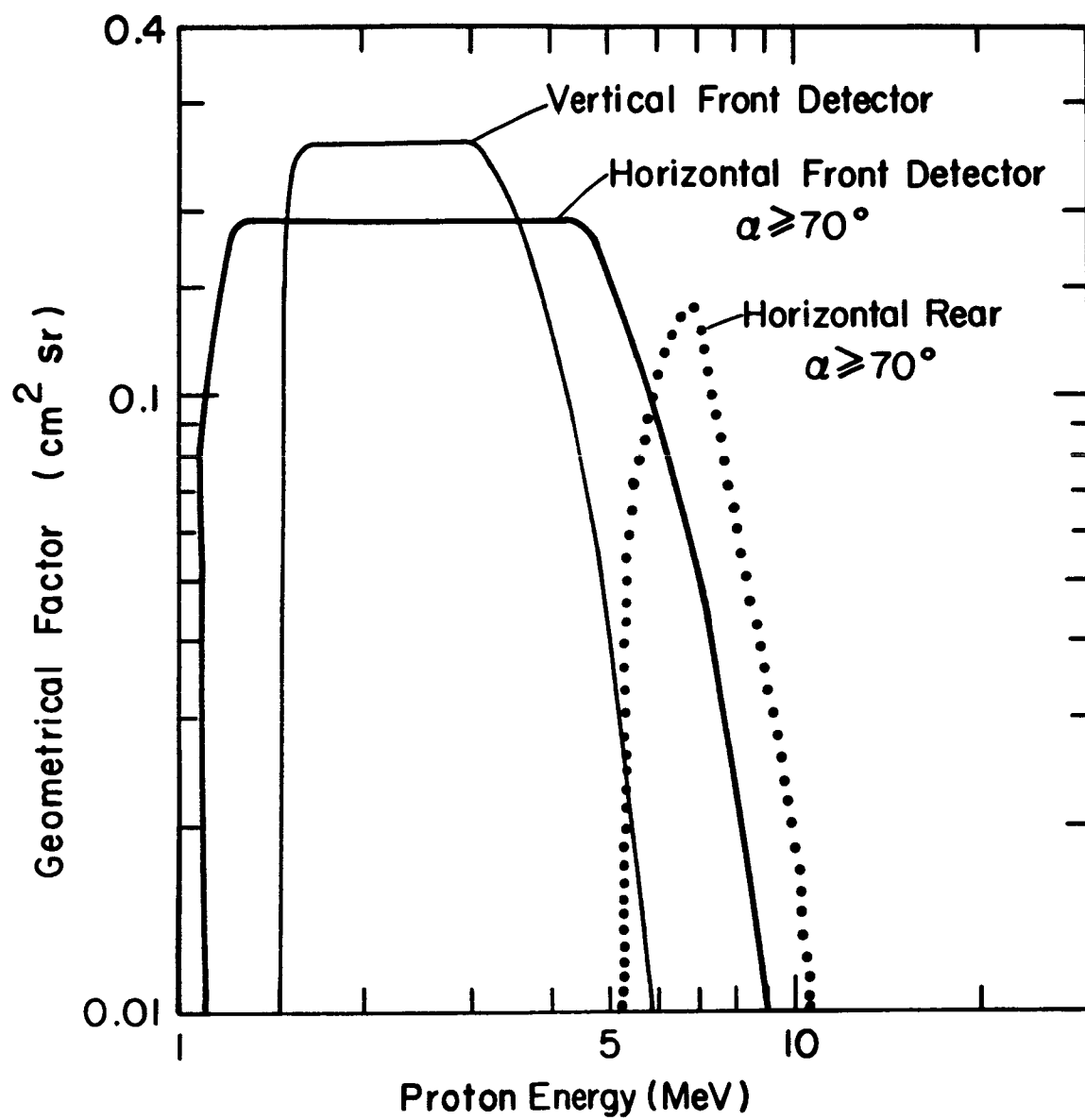


Fig. 4

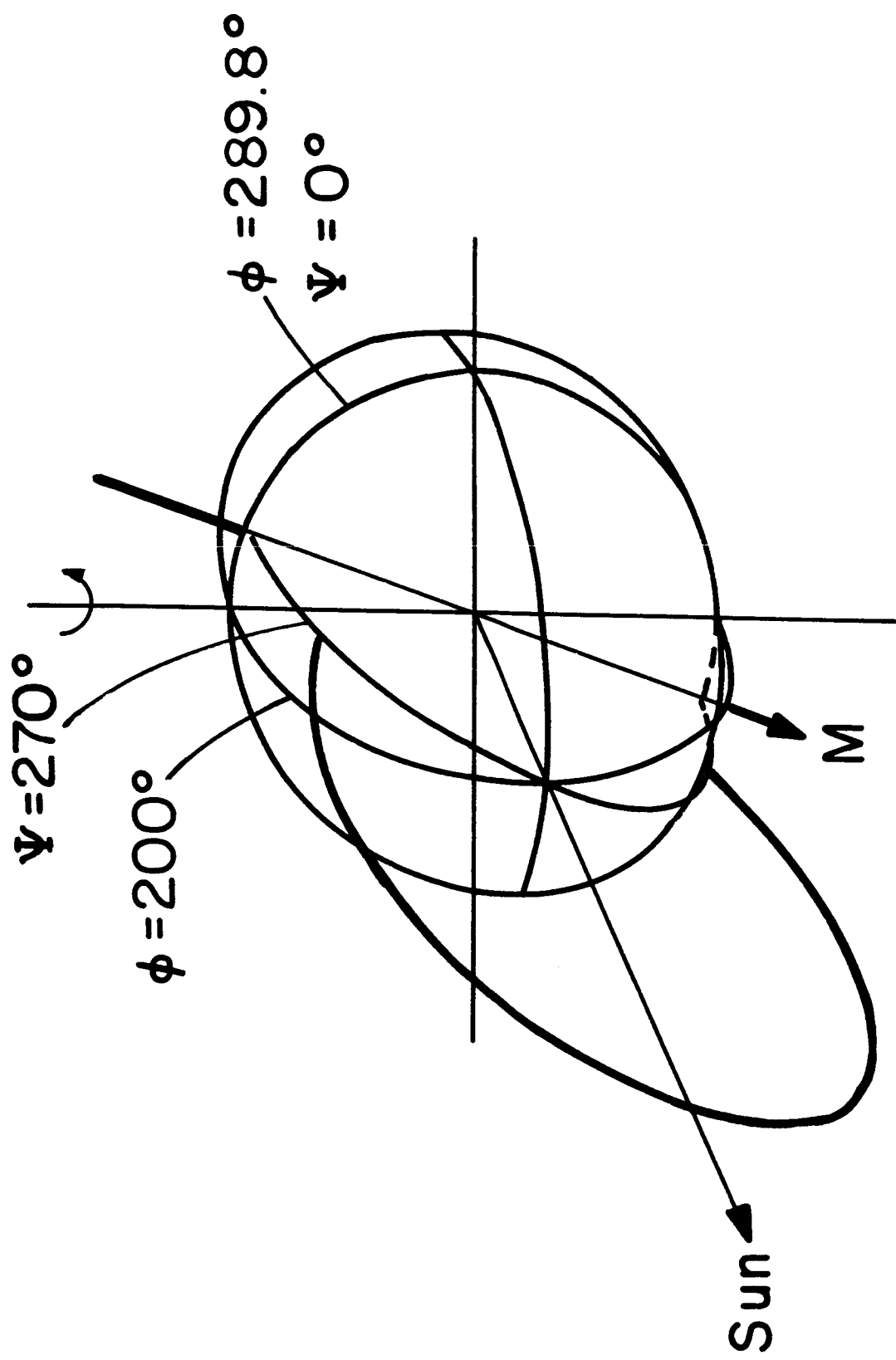


Fig.5

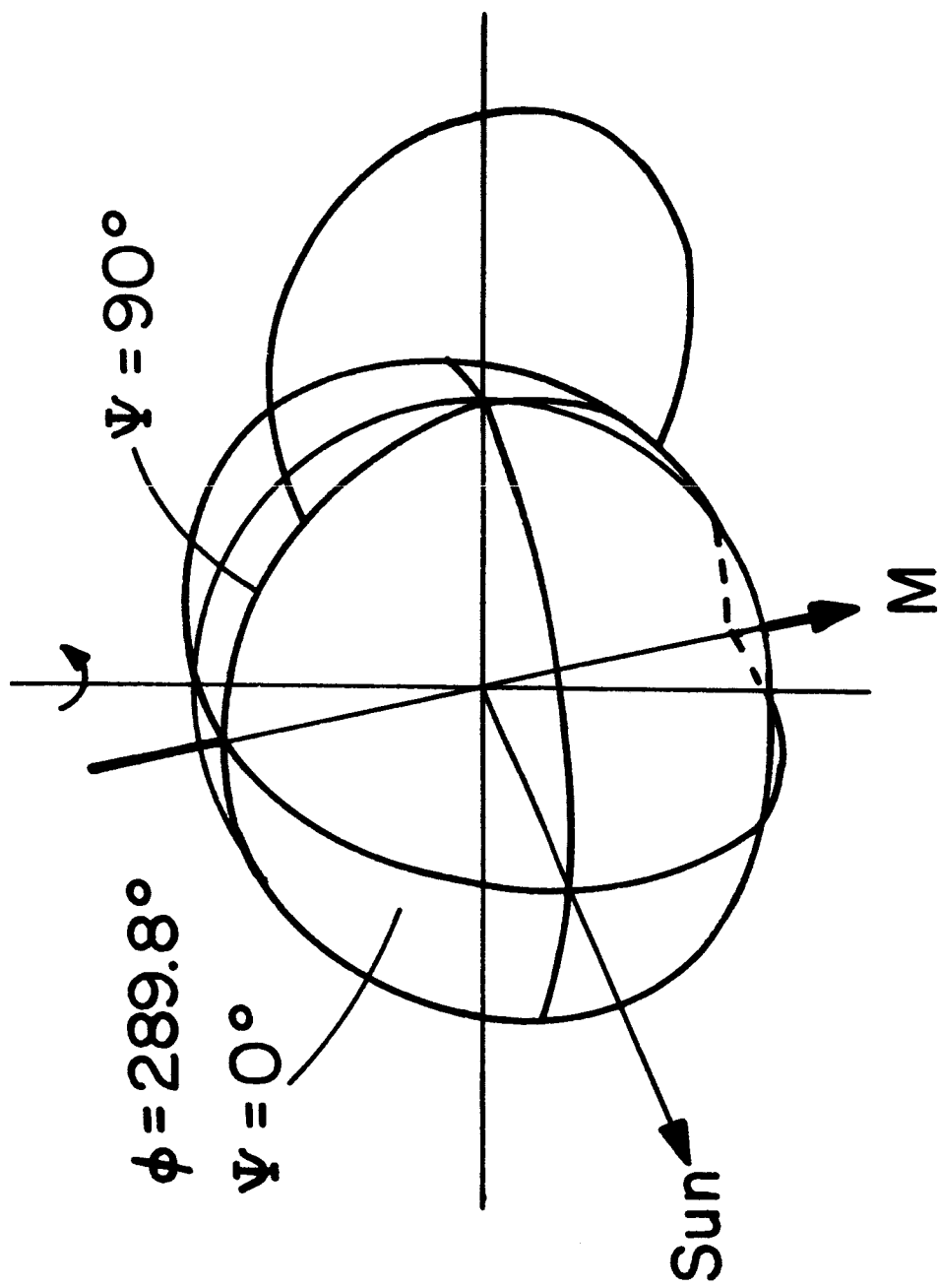


Fig. 6

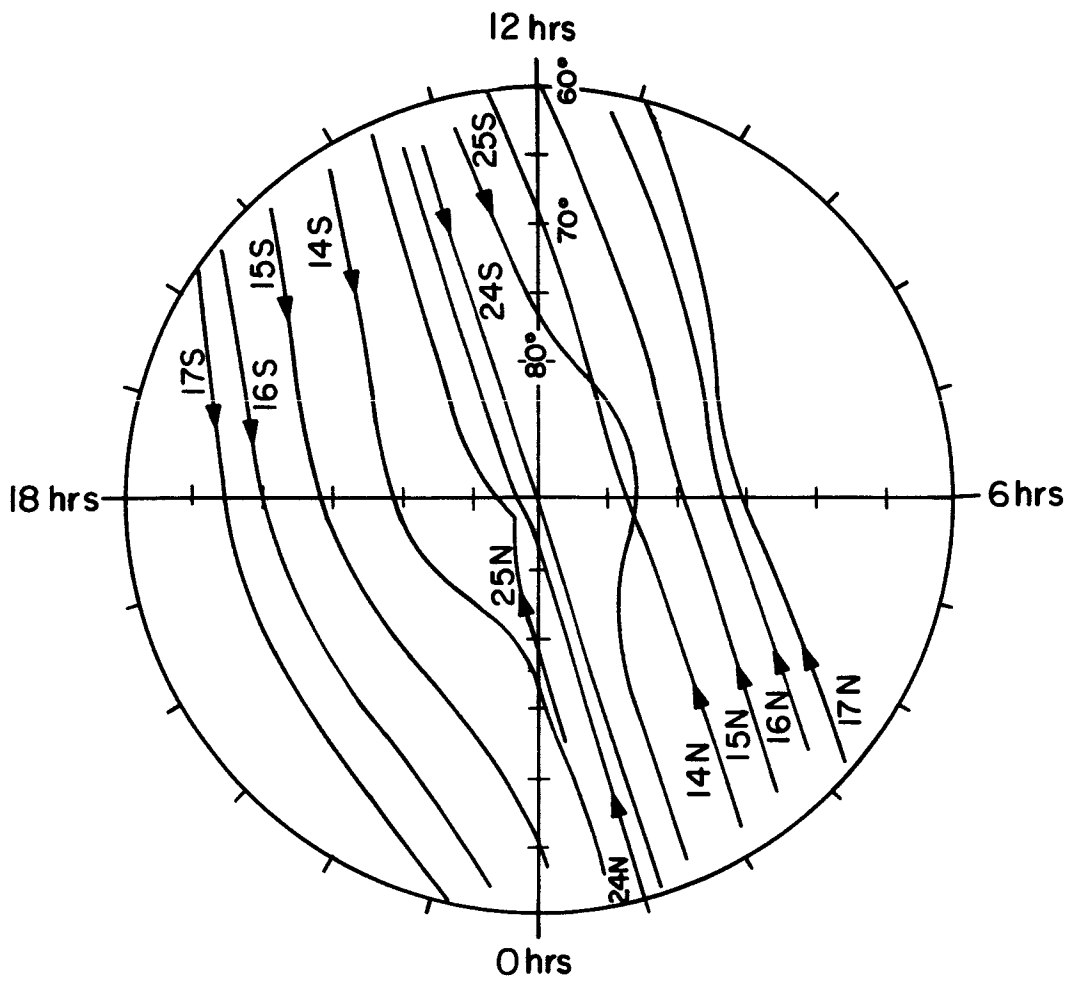


Fig.7

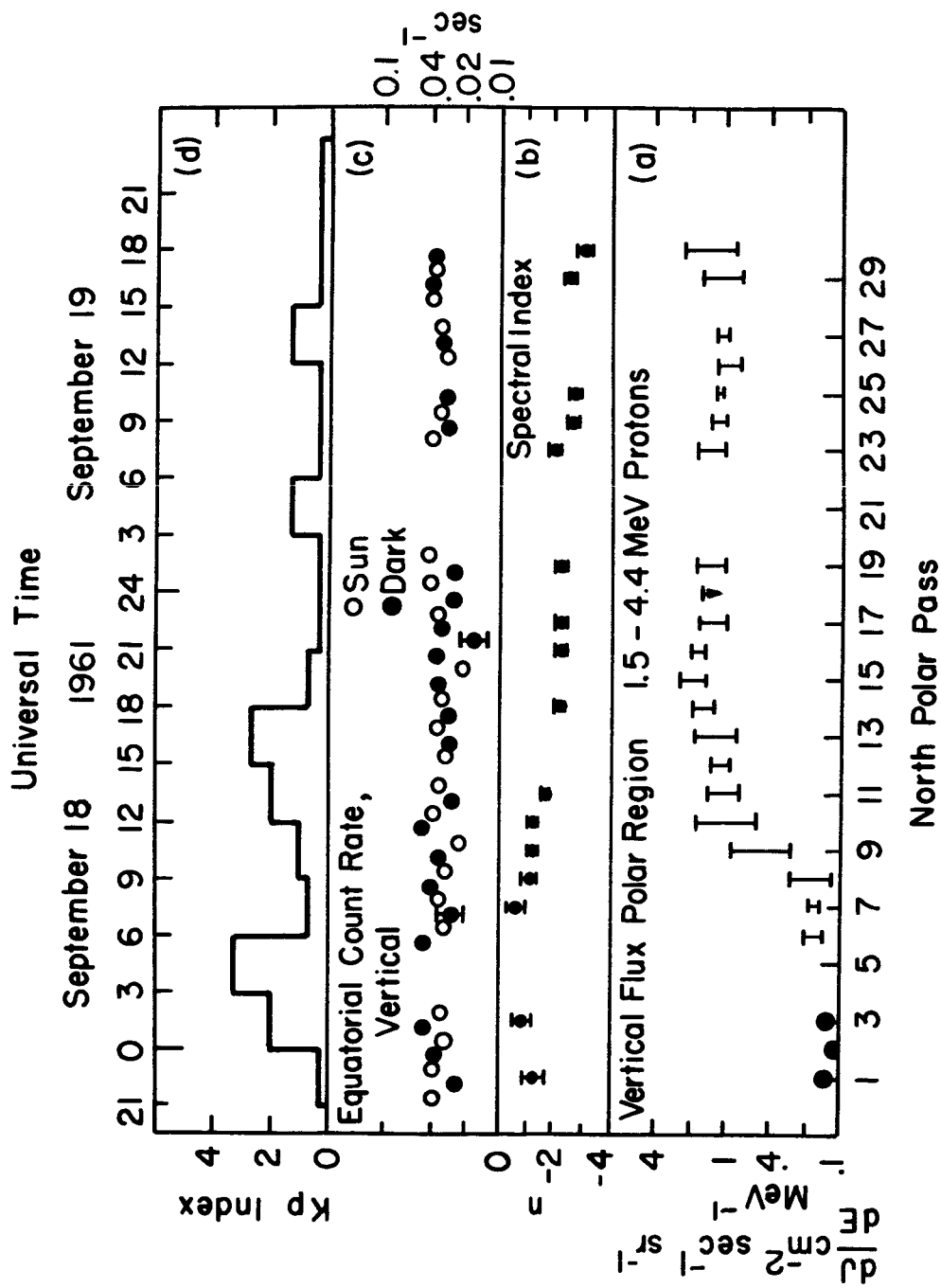


Fig.8

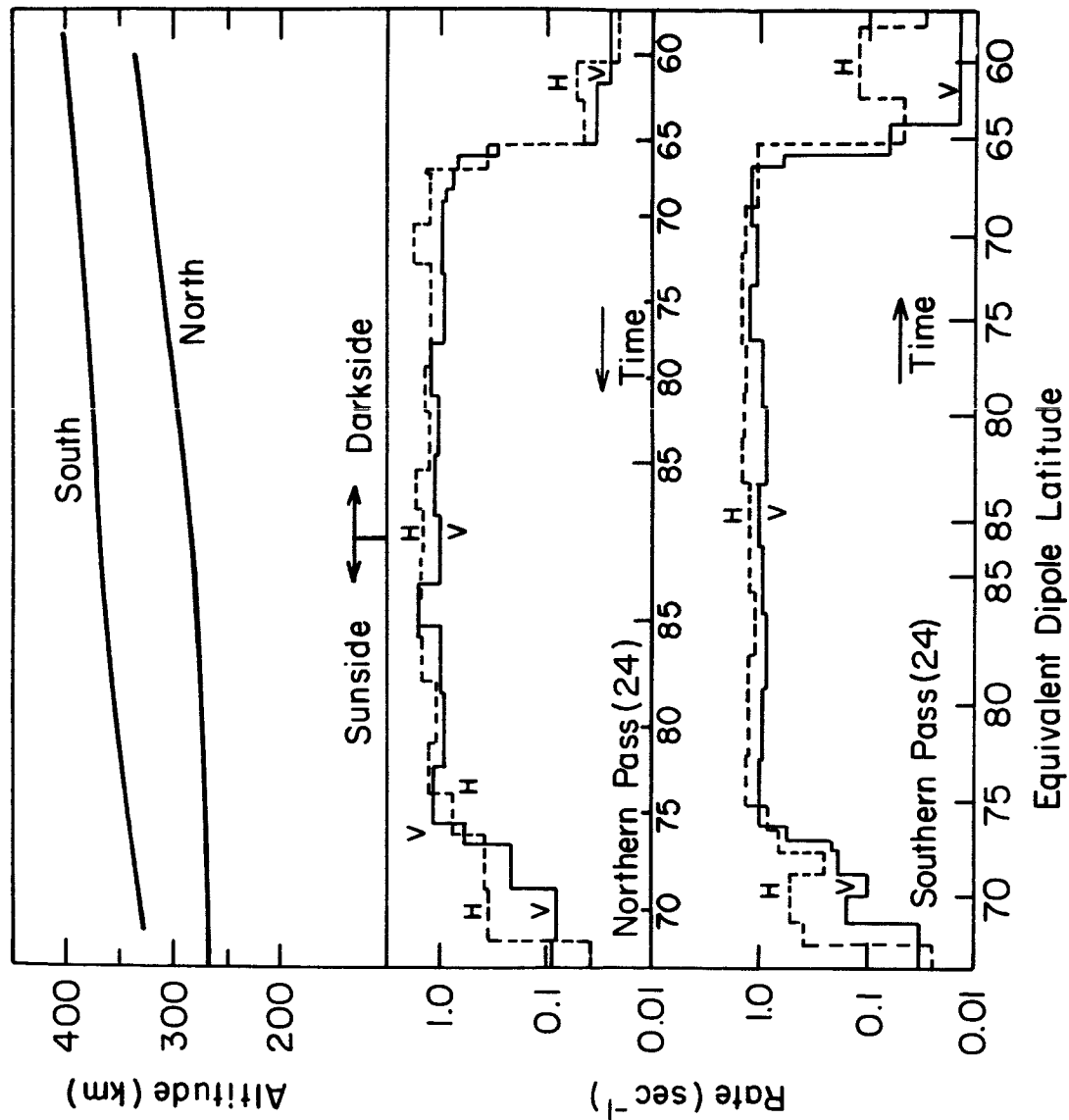


Fig.9

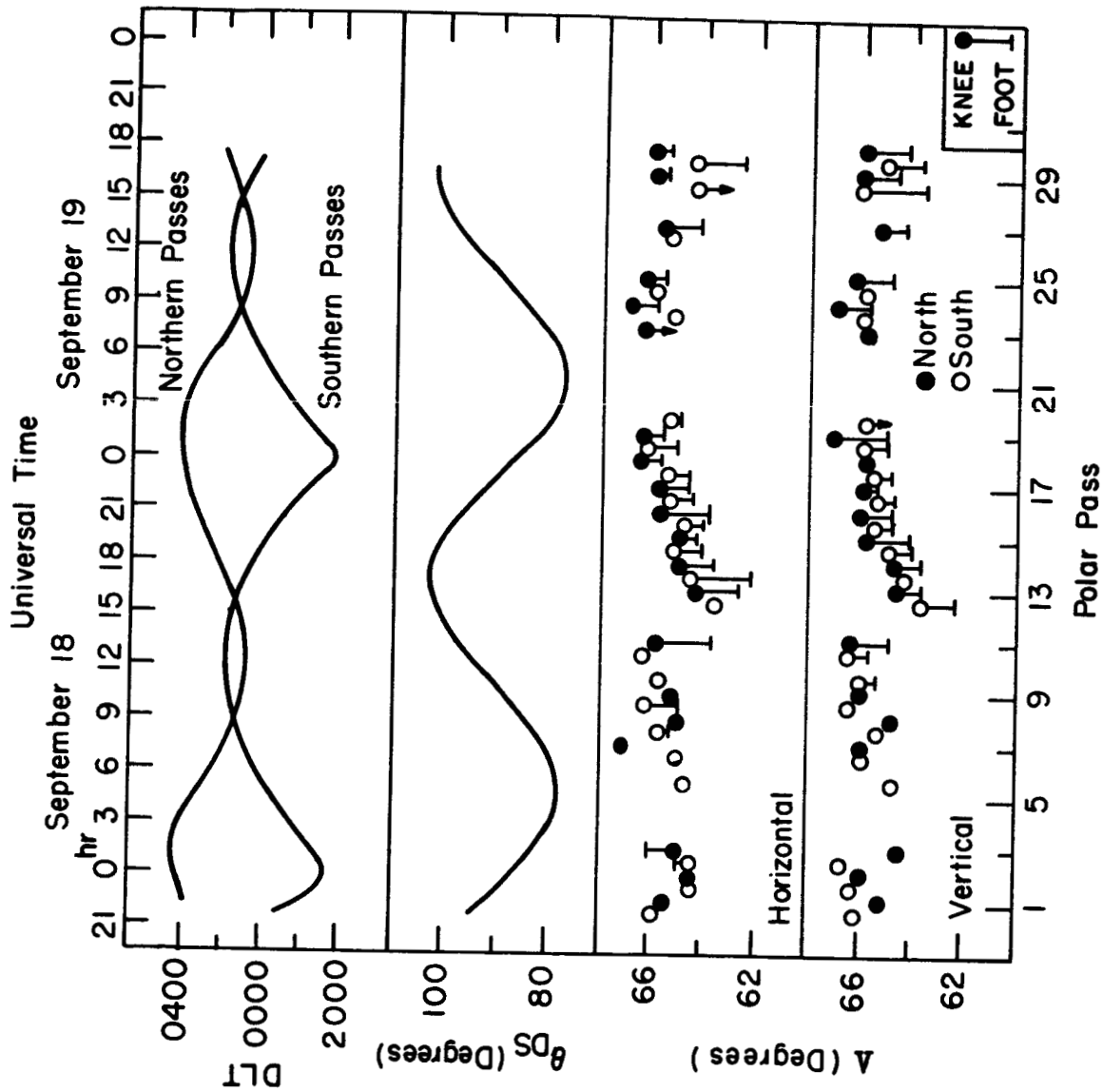


Fig. 10

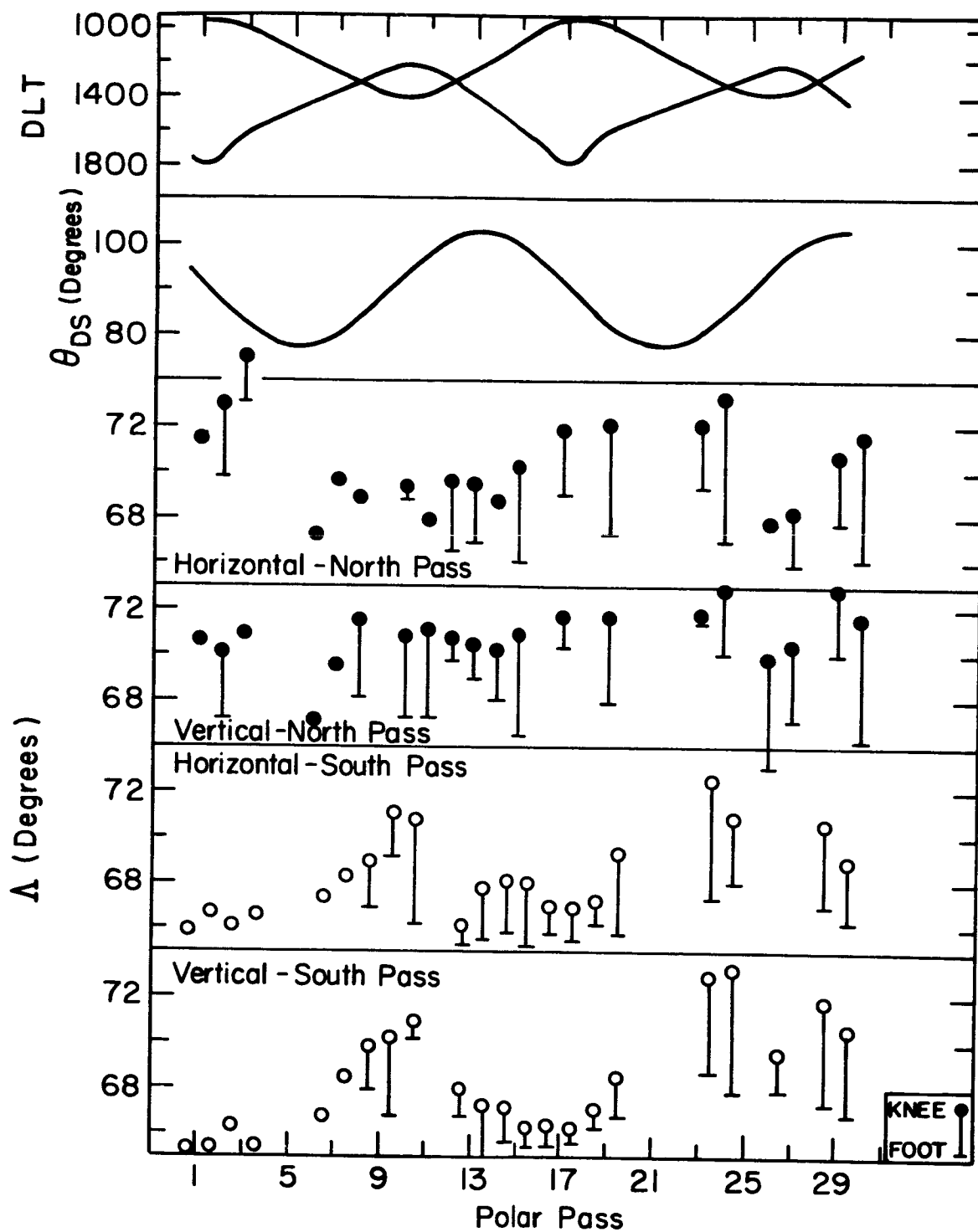


Fig. 11

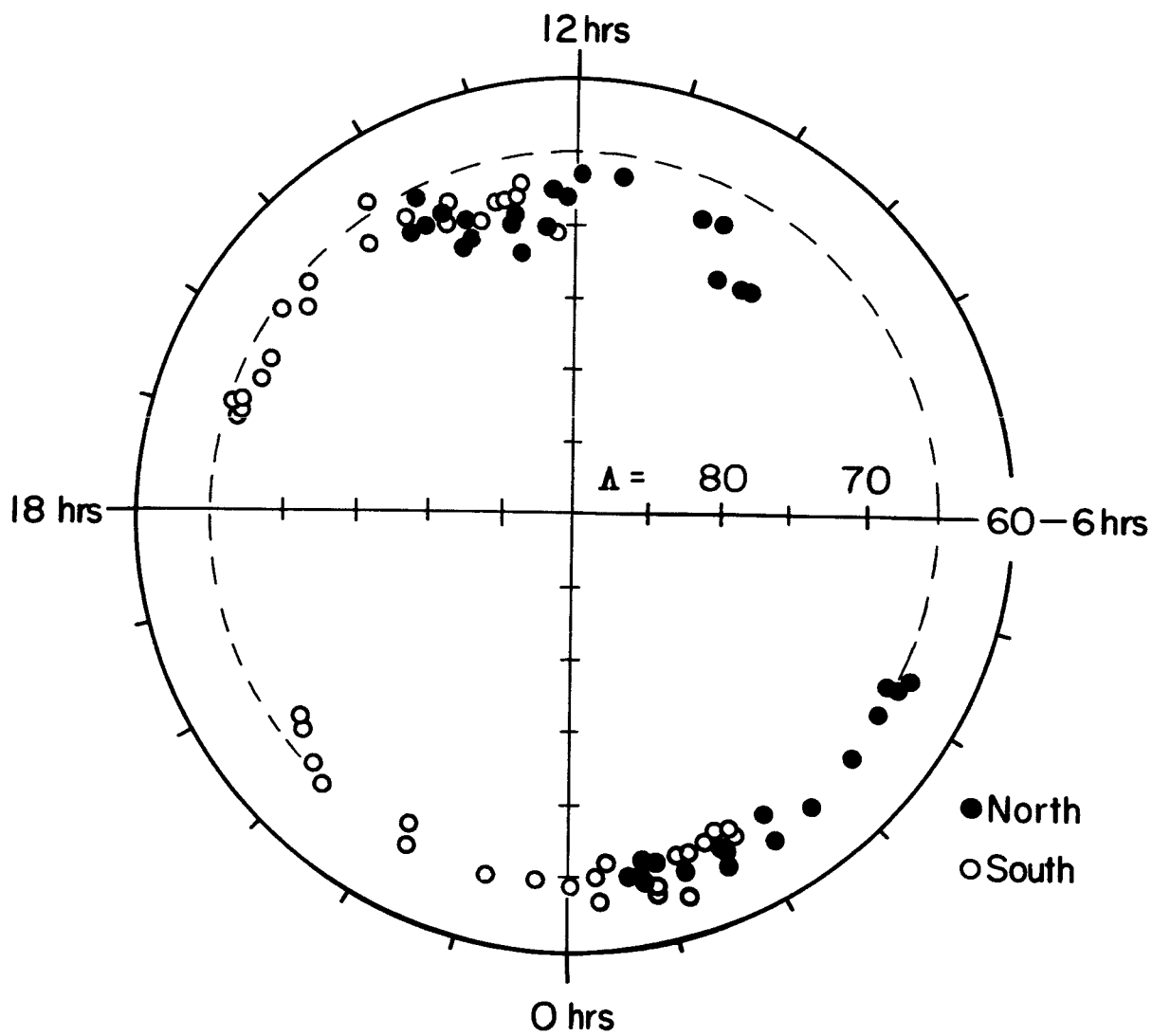


Fig.12

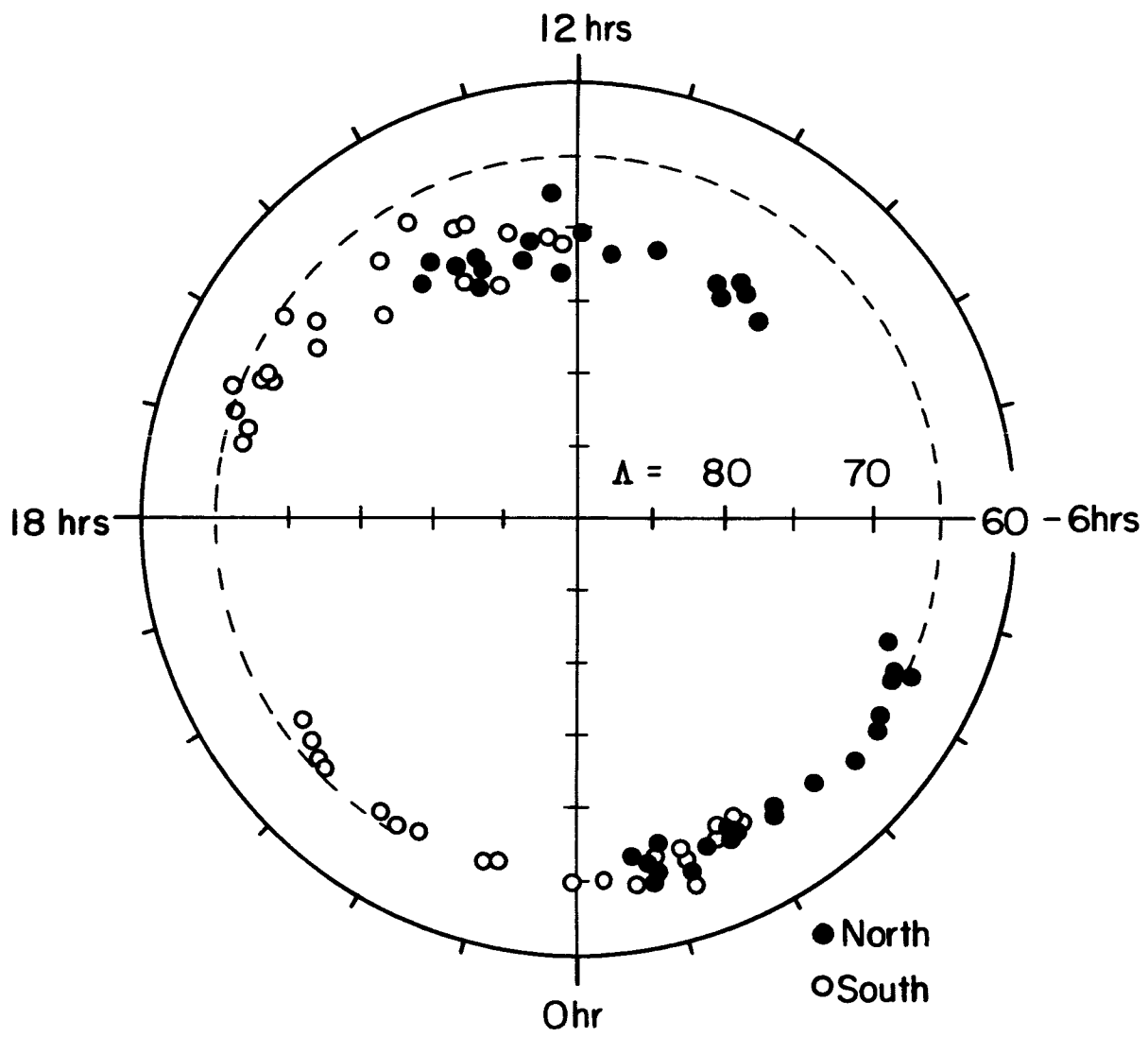


Fig.13

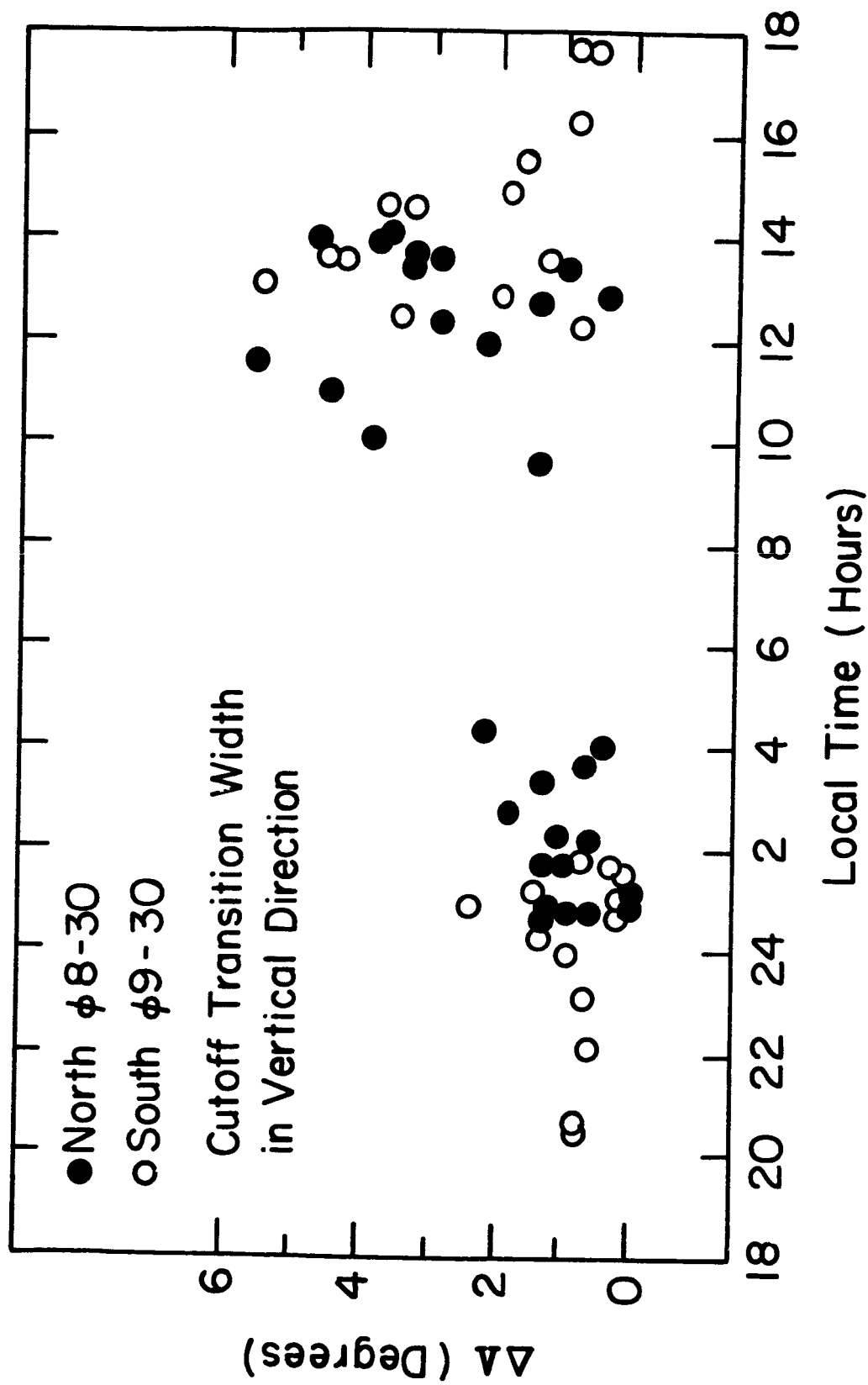


Fig.14